

## Nuclear-Structure Dependence of Heavy-Ion-Fusion Partial-Wave Distributions

W. Kühn, A. Ruckelshausen, R. D. Fischer, G. Breitbach, H. J. Hennrich, V. Metag, and R. Novotny

*II. Physikalisches Institute, Universität Giessen, Giessen, West Germany*

R. V. F. Janssens and T. L. Khoo

*Argonne National Laboratory, Argonne, Illinois 60439*

D. Habs and D. Schwalm

*Max-Planck-Institut für Kernphysik, Heidelberg, West Germany, and  
Physikalisches Institut, Universität Heidelberg, Heidelberg, West Germany*

B. Haas

*Centre de Recherches Nucléaires, Strasbourg, France*

R. S. Simon

*Gesellschaft für Schwerionenforschung, Darmstadt, West Germany*

(Received 5 December 1988).

Partial-wave cross sections for fusion of  $^{64}\text{Ni} + ^{92}\text{Zr}$  and  $^{64}\text{Ni} + ^{96}\text{Zr}$  at energies of 5% and 7% above the Bass-model fusion barrier have been measured with the Darmstadt-Heidelberg Crystal Ball. The distribution for fusion with the more neutron-deficient target  $^{92}\text{Zr}$  exhausts the unitarity limit for lower angular momenta. In contrast, fusion with the slightly more neutron-rich target  $^{96}\text{Zr}$  yields a broad angular momentum distribution with cross sections well below unitarity even for small partial waves.

PACS numbers: 25.70.Jj, 25.70.Gh, 27.70.+q

The discovery<sup>1</sup> of enhanced sub-barrier fusion cross sections and its subsequent interpretation<sup>2-4</sup> in terms of coupling to binary reaction channels has renewed the interest in near-barrier heavy-ion-fusion studies. Yet, there are still many open questions and problems related to the fusion process and to the subsequent decay of the fusion product, the compound nucleus. This is partly due to experimental difficulties which until recently did not permit a direct and unambiguous measurement of the partial-wave cross sections for heavy-ion fusion. The knowledge of the compound-nucleus angular momentum distribution is of crucial importance for an understanding of the fusion process itself, in particular near the barrier. Moreover, the excitation-energy and angular momentum distribution determine the decay properties of the compound nucleus. Recently, new techniques involving  $4\pi$   $\gamma$ -detector systems such as the Darmstadt-Heidelberg Crystal Ball<sup>5</sup> have been developed which permit a novel access to the fusion process by directly measuring angular momentum distributions of fusion products.<sup>6</sup>

This Letter presents the first direct comparison of measured partial-wave distributions for systems with similar reaction dynamics but different nuclear structure. The systems investigated are  $^{64}\text{Ni} + ^{92}\text{Zr} \rightarrow ^{156}\text{Er}$  at a center-of-mass energy of  $E_{c.m.} = 138.8$  MeV (5% above the Bass-model<sup>7</sup> fusion barrier) and  $^{64}\text{Ni} + ^{96}\text{Zr} \rightarrow ^{160}\text{Er}$  at  $E_{c.m.} = 139.5$  MeV (7% above the Bass barrier).

Isotopically enriched targets of  $^{92}\text{Zr}$  (95%, 320  $\mu\text{g}/\text{cm}^2$ ) and  $^{96}\text{Zr}$  (85%, 200  $\mu\text{g}/\text{cm}^2$ ) were irradiated

with  $^{64}\text{Ni}$  beams provided by the Max-Planck-Institut tandem postaccelerator facility at Heidelberg. The  $\gamma$  radiation from the residual nuclei was registered in 158 NaI modules of the Crystal Ball and in one Ge detector. Time of flight with respect to the pulsed beam was used to discriminate  $\gamma$  rays and neutrons in the NaI detectors.

The primary information obtained from the Crystal Ball is a distribution of the number of responding detectors. This distribution is obtained separately for each individual decay channel selected by gates on discrete lines in the germanium-detector  $\gamma$ -energy spectrum. After correcting for the Crystal Ball response,  $\gamma$  multiplicity distributions are obtained. The average spin removed per  $\gamma$  ray has been determined by two independent methods. Method A is based on an analysis of the  $\gamma$ -ray angular distribution<sup>8</sup> while method B determines the average spin per  $\gamma$  ray from the ratio of discrete dipole and quadrupole transitions observed in the germanium-detector spectrum.<sup>9,10</sup> Both methods, which yield consistent results within errors, are used to convert multiplicity distributions into angular momentum distributions for the individual evaporation residues.

As a final correction, the angular momentum carried away by neutron and light-charged particle evaporation prior to  $\gamma$  emission has to be taken into account. For the reactions discussed here, this is only a minor contribution which can be estimated from statistical model calculations.

Angular momentum distributions for individual decay channels are derived by gating on specific lines in the Ge

detector. The individual contributions are then summed, with the relative strengths determined from the Ge spectra. The absolute normalization is taken from independent measurements<sup>11-13</sup> of the evaporation-residue cross sections. The above procedure is described in more detail in Refs. 6 and 8. The methods used here are not applicable to fusion followed by fission. In the following the term "fusion" refers to the part of the compound-nucleus formation cross section leading to evaporation residues only.

Figure 1 compares the compound-nucleus partial-wave distributions for the reactions  $^{64}\text{Ni} + ^{92}\text{Zr} \rightarrow ^{156}\text{Er}$  and  $^{64}\text{Ni} + ^{96}\text{Zr} \rightarrow ^{160}\text{Er}$ . The more neutron-deficient system  $^{64}\text{Ni} + ^{92}\text{Zr} \rightarrow ^{156}\text{Er}$  (top) exhibits an almost triangular partial-wave distribution as expected in standard barrier penetration models. In contrast, the slightly more neutron-rich system  $^{64}\text{Ni} + ^{96}\text{Zr} \rightarrow ^{160}\text{Er}$  (bottom) shows a very broad spin distribution ranging to higher partial waves.

Figure 1 exhibits another striking difference: The sys-

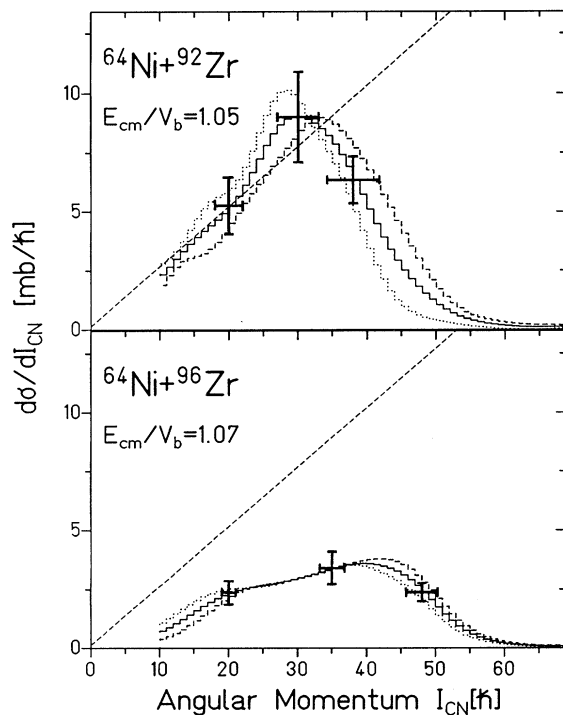


FIG. 1. Compound-nucleus angular momentum distributions for  $^{64}\text{Ni} + ^{92}\text{Zr} \rightarrow ^{156}\text{Er}$  (top) and  $^{64}\text{Ni} + ^{96}\text{Zr} \rightarrow ^{160}\text{Er}$  (bottom). The dotted histograms are obtained by method A to convert multiplicity into spin. For the dashed histograms, the conversion was done with method B. The solid histogram is obtained from average conversion factors of both methods. Typical error bars including both statistical and systematic errors are indicated. The dashed lines represent the unitarity limit. No data are shown for spins less than  $10\hbar$  because of systematic deficiencies in the multiplicity to spin conversion (see Ref. 6).

tem  $^{64}\text{Ni} + ^{92}\text{Zr} \rightarrow ^{156}\text{Er}$  exhausts the unitarity limit (dashed line) at the lower angular momenta, while for  $^{64}\text{Ni} + ^{96}\text{Zr} \rightarrow ^{160}\text{Er}$  the partial cross sections are significantly below the unitarity limit even for low partial waves. An alternative way to demonstrate the differences between the two systems is shown in Fig. 2, where the fusion probability  $T_l$  for a partial wave with angular momentum  $l$  given by

$$T_l = \frac{\sigma_{\text{fusion}}(l)}{\pi\lambda^2(2l+1)}, \quad (1)$$

where  $\lambda$  is the de Broglie wavelength. The difference between the two systems is quite unexpected. The low  $T_l$ 's for the more neutron-rich system are due to the rather low evaporation-residue cross section of  $133 \pm 25$  mb observed at  $1.07V_B$ .<sup>12</sup> In comparison, a cross section of  $239 \pm 36$  mb has been reported for the system  $^{64}\text{Ni} + ^{92}\text{Zr}$  at  $1.05V_B$ .<sup>13</sup> The low evaporation-residue cross section for  $^{64}\text{Ni} + ^{96}\text{Zr}$  implies that other reaction channels successfully compete with fusion even at low partial waves. A cross-sectional measurement of these other channels, together with a reconfirmation of the small fusion cross section of Ref. 12, would be desirable.

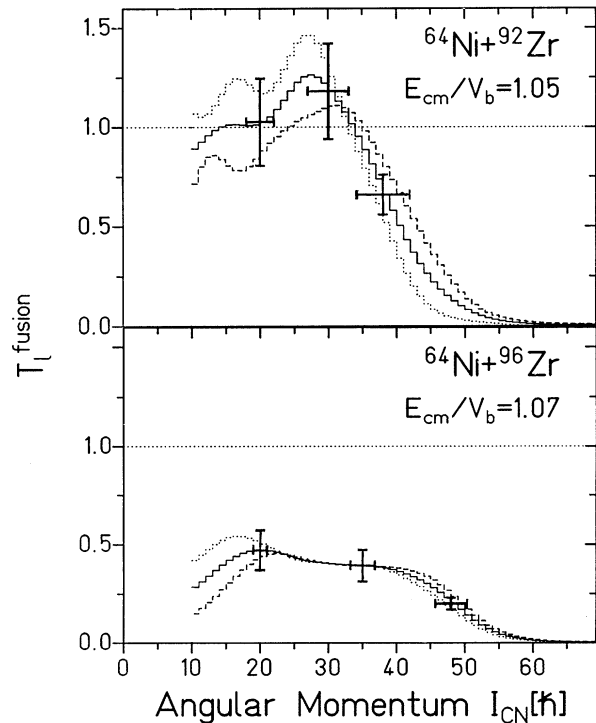


FIG. 2. Deduced fusion probabilities for  $^{64}\text{Ni} + ^{92}\text{Zr} \rightarrow ^{156}\text{Er}$  (top) and  $^{64}\text{Ni} + ^{96}\text{Zr} \rightarrow ^{160}\text{Er}$  (bottom). Dotted and dashed histograms are obtained using methods A and B, respectively, for a conversion of multiplicity into spin. The solid histogram is obtained from average conversion factors of both methods. Typical error bars including both statistical and systematic errors are indicated.

An arbitrary rescaling of the angular momentum distribution such that unitarity is reached at low partial waves for  $^{64}\text{Ni} + ^{96}\text{Zr}$  would lead to a total evaporation-residue cross section of 295 mb, which is more than twice as large as the experimental value of Ref. 12.

Since the entrance channel mass asymmetry degree of freedom and the incident energy are almost identical for both systems, the observed differences in the angular momentum distributions could be due to an effective increase in the fusion barrier caused by changes in the nuclear structure of the Zr targets with increasing neutron number. Large shifts in the effective fusion barrier have also been observed<sup>14</sup> in excitation functions for fusion of various combinations of Zr isotopes with beams of  $A \sim 90\text{--}100$ . With increasing neutron number, the experimental fusion barrier, defined as the energy where the fusion probability reaches 0.5, systematically shifts towards higher energies, as compared to the Bass-model barrier. On the other hand, the Bass barrier is equal to the experimental barrier for the closed-shell system  $^{90}\text{Zr} + ^{90}\text{Zr}$ .

If a similar phenomenon were to occur for the systems investigated here, the reaction  $^{64}\text{Ni} + ^{92}\text{Zr}$  would correspond to fusion above the "true" fusion barrier, leading to an angular momentum distribution exhausting unitarity for the lower partial waves. In contrast, the more neutron-rich target  $^{96}\text{Zr}$ , which seems to show an effective increase of the barrier, would then correspond to a case of sub-barrier fusion. This may provide a plausible explanation for the measured broad angular momentum distribution, which is a typical feature of sub-barrier fusion.

In summary, partial-wave cross sections for near-barrier fusion have been measured with a modular  $4\pi$   $\gamma$  detector. Striking differences in the partial-wave distri-

butions for systems with comparable reaction dynamics but different nuclear structure have been observed, which can be related to a possible increase of the effective fusion barrier.

We are grateful to H. Folger and the Gesellschaft für Schwerionenforschung target laboratory staff for preparing the excellent targets. We would also like to thank E. Jaeschke, R. Repnow, and the operator staff of the Heidelberg tandem postaccelerator facility for delivering the Ni beam. One of us (T.L.K.) acknowledges the hospitality of the Max-Planck-Institut für Kernphysik, Heidelberg. This work was supported in part by Gesellschaft für Schwerionenforschung and Deutsches Bundesministerium für Forschung und Technologie, and by the U.S. Department of Energy under Contract No. W-31-109-ENG.38.

- 
- <sup>1</sup>M. Beckerman, Phys. Rep. **129**, 145 (1985).
  - <sup>2</sup>H. Esbensen, Nucl. Phys. **A352**, 147 (1980).
  - <sup>3</sup>S. Landowne and C. H. Dasso, Phys. Lett. B **138**, 32 (1984).
  - <sup>4</sup>W. Reisdorf *et al.*, Nucl. Phys. **A438**, 212 (1985).
  - <sup>5</sup>V. Metag *et al.*, in *Detectors in Heavy-Ion Reactions*, edited by W. von Oertzen, Lecture Notes in Physics Vol. 178 (Springer-Verlag, Berlin, 1983) p. 163.
  - <sup>6</sup>R. D. Fischer *et al.*, Phys. Lett. B **171**, 33 (1986).
  - <sup>7</sup>R. Bass, Nucl. Phys. **A231**, 45 (1974).
  - <sup>8</sup>A. Ruckelshausen *et al.*, Phys. Rev. Lett. **56**, 2356 (1986).
  - <sup>9</sup>D. J. G. Love *et al.*, Phys. Rev. Lett. **57**, 551 (1986).
  - <sup>10</sup>A. Ruckelshausen *et al.*, Phys. Rev. Lett. **58**, 1584 (1987).
  - <sup>11</sup>G. Duchéne, Ph.D. thesis, University of Strasbourg, 1985 (unpublished).
  - <sup>12</sup>B. Haas *et al.*, Phys. Rev. Lett. **54**, 398 (1985).
  - <sup>13</sup>R. V. F. Janssens *et al.*, Phys. Lett. B **181**, 16 (1986).
  - <sup>14</sup>J. G. Keller *et al.*, Nucl. Phys. **A452**, 173 (1986).